

Autologous tumor cell immunotherapeutic platform induces stress-correlated immunogenic cell death leading to immune activation within the draining lymph nodes

Christopher Cultrara¹, Kenneth Kirby¹, Essam Elrazaq¹, Christopher Uhl¹, Amelia Zellander¹, Lorenzo Galluzzi², Mark A. Exley¹, Jenny Zilberberg¹

BACKGROUND

Imvax, Inc. is developing a novel personalized immunotherapeutic platform combining irradiated patient-derived tumor cells and insulin-like growth factor type-1 receptor antisense oligonucleotide (IMV-001) in biodiffusion chambers (BDCs; 0.1-micron pores). The glioblastoma (GBM) drug-device combination product, IGV-001, was evaluated in a newly diagnosed GBM phase 1b clinical trial¹. Median overall survival of highest exposure IGV-001-treated 'Stupp-eligible'² patients (n=10) was 38.2 months compared with 16.2 months in recent standard-of-care-treated patients (P=0.044)¹ [NCT02507583]. Imvax also reported anti-tumor activity of IGV-001 in the GL261-Luc intracranial GBM murine model³. Here, we show that *m*IGV-001 (prepared with murine GL261 cells) is associated with activation of stress-related pathways and the release of immunogenic cell death (ICD)⁴ molecules capable of stimulating myeloid and T cell subsets with potential anti-tumor activity in the draining lymph nodes (dLNs) proximal to the BDC.

METHODOLOGY

*m*IGV-001 was incubated at 37°C and 5% CO₂ for 48 h as shown in **Figure 1**. BDC contents were analyzed for extracellular ATP (eATP) using a luciferase bioluminescent system and high mobility group box 1 (HMGB1) protein via ELISA, as indicators of ICD. Reactive oxygen species (ROS) accumulation was determined by flow cytometry as well as cell viability via Annexin V and 7-AAD analysis. Changes in stress-related apoptotic signaling pathways were analyzed by immunoblotting. dLNs from mice receiving *m*IGV-001 and s.c. tumor-challenge with GL261-luc cells were isolated for immunophenotyping.

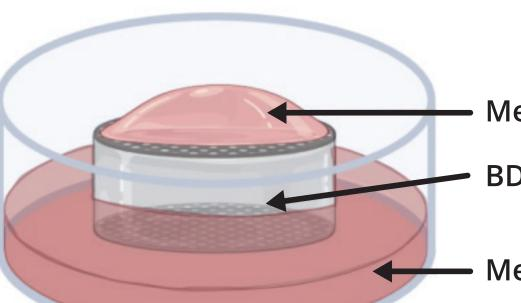
FIGURE 1



In vitro BDC Culture Assay

In vitro Minimal Media

12 Well Plate



Media on top of BDC (200 µl)

Side View

5 mm

Media below BDC (500 μl)

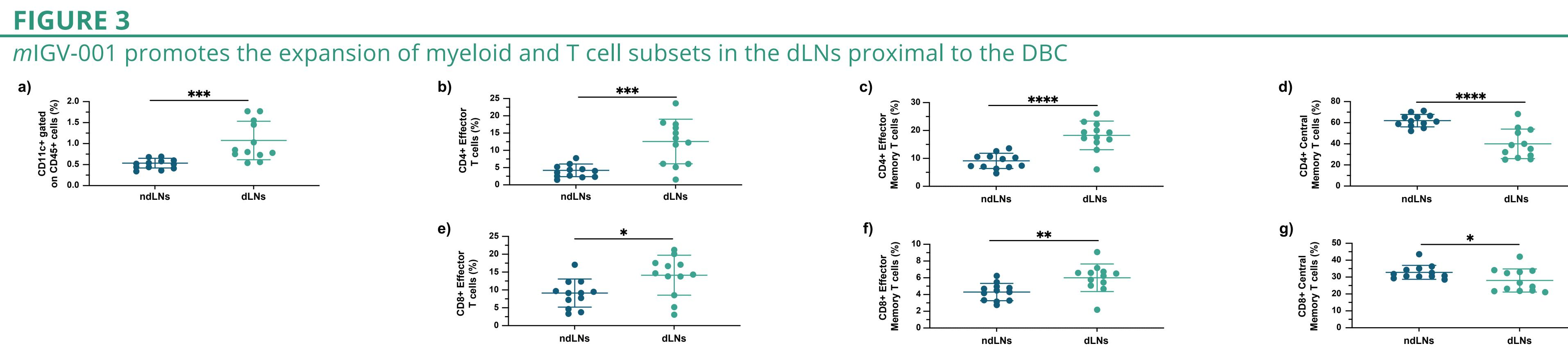
RESULTS

- *vitro* (fig. 4).

FIGURE 2



Mice were treated with *m*IGV-001 BDC or PBS-loaded BDC (i.e., Control BDC) for 48 h prior to explantation. Mice received tumor challenge 28 days later and monitored for disease progression and survival for a further 60 days. **a)** Kaplan-Meier survival curves, data combined from 2 separate experiments. Log-Rank test, **** P<0.0001.



a)		
-	(%)	2.0 –
	D11c+ gated D45+ cells (⁹	1.5 -
	то т	1.0 —
	CD11c+ on CD45+	0.5
	uo	0.0

BDC's dLN and non-draining LN (ndLN) were isolated from 12 mice and analysis to compare the distribution of myeloid and T cell subsets. a) Percentage of CD11c+ cells. **b)** Percentage of CD4+CD62L-CD44- effector T cells. **c)** Percentage of CD4+CD62L+CD44+ central memory T cells. **e)** Percentage of CD8+CD62L-CD44- effector T cells. f) Percentage of CD8+CD62L-CD44+ effector memory T cells. g) Percentage of CD8+CD62L+CD44+ central memory T cells. Statistical analysis was performed using unpaired t-test, **** P<0.0001, *** P<0.001, ** P=0.0061, * P<0.05.

• *m*IGV-001 treated mice exhibit substantially longer median survival time compared to control animals in the GL261-Luc intracranial GBM model (fig. 2). • Phenotyping analyses showed increased CD45+CD11b+CD11c+MHCII+ DCs in the dLNs compared to the contralateral control site without BDC. Likewise, the percentage of effector and effector memory in CD4+ and CD8+ T cells was also significantly higher in the dLNs (fig. 3), as were CD8+TIM3+, CD8+PD1+, and CD4+PD1+ T cells (data not shown).

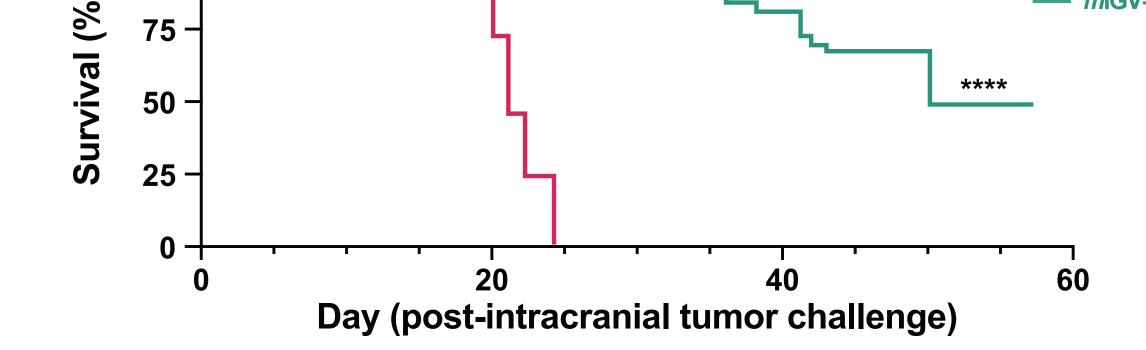
• Cells in *m*IGV-001 released eATP after formulation and eATP was detectable within the BDCs over 48 h (fig. 4).

• HMGB1 was released from dying tumor cells in *m*IGV-001 (fig. 4), while surface calreticulin was undetectable (data not shown).

• Similar levels of cell death and HMGB1 release were observed *in vivo* and *in*

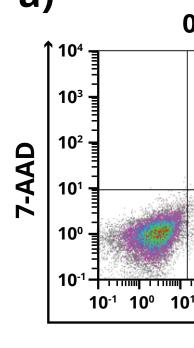
• Immunoblot analysis showed induction of the integrated stress response (ISR) pathway via eif 2α activation and upregulation of the ATF4-CHOP axis (fig. 5). • ROS levels were elevated after 24 h with subsequent activation of the JNK pathway, downregulation of the anti-apoptotic marker BCL-2, and increased activity of the apoptotic effector caspase-3/7 (fig. 5).

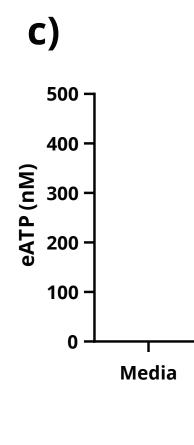
*m*IGV-001 extends the survival of GBM-bearing mice in the GL261-Luc intracranial GBM murine model **≥** 75 -

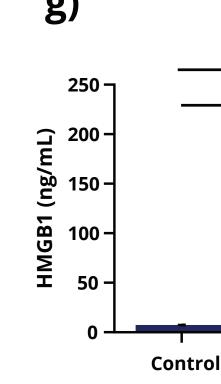






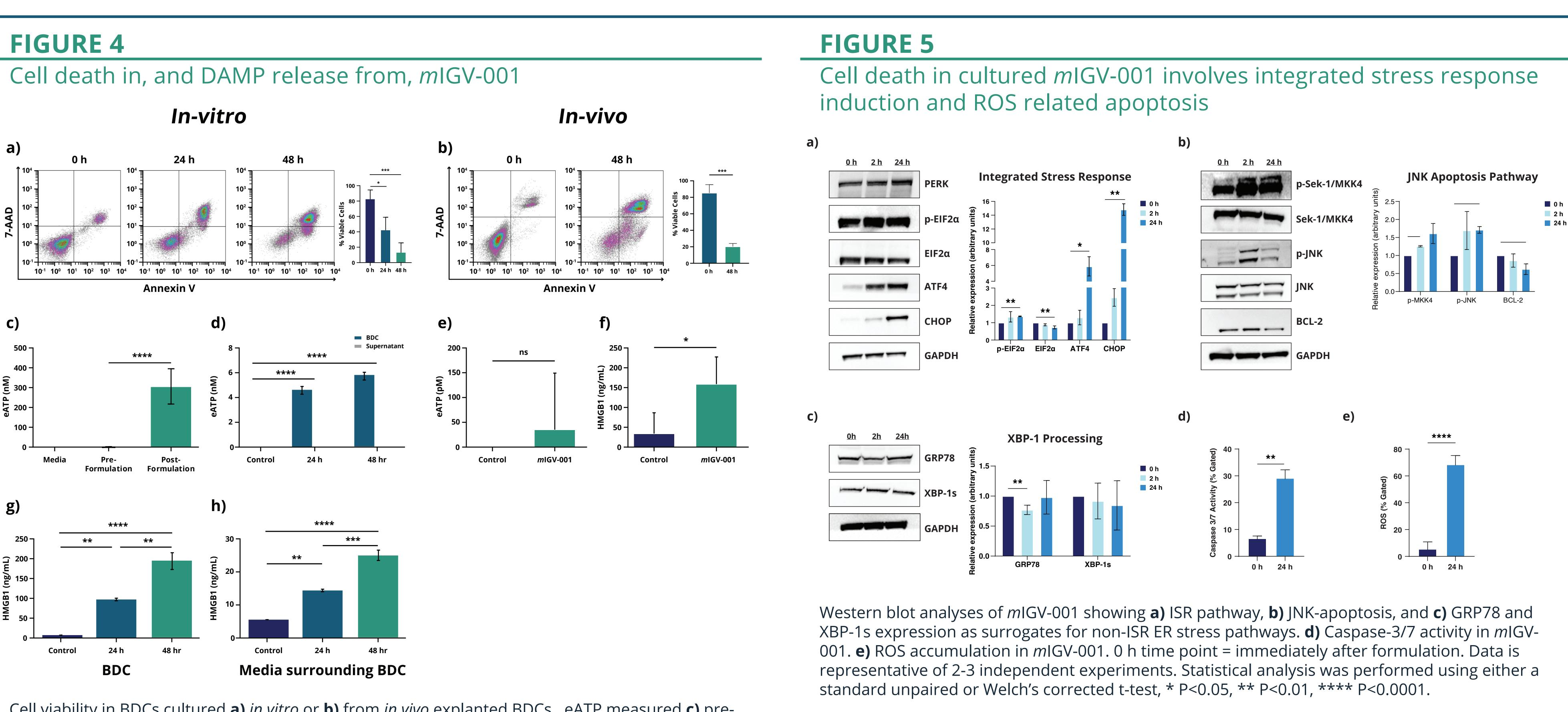






Cell viability in BDCs cultured **a)** in vitro or **b)** from in vivo explanted BDCs. eATP measured **c)** preand post-formulation, **d)** in BDC supernatants and released into the culture medium over time *in vitro*, and **e**) within *in vivo* explanted BDC supernatant. HMGB1 measured **f**) in explanted BDC supernatant or **g-h)** HMGB1 measured in BDCs cultured *in vitro* and released into the culture medium over time. Data is representative of 2-3 independent *in vitro* experiments and 3-12 mice for *in vivo* data. Control = PBS-filled BDC. *In vivo* HMGB1 data was normalized to surgical controls. Statistical analysis was performed using One-way Anova with multiple comparisons or unpaired t-test, * P<0.05, ** P<0.01, *** P<0.001, **** P<0.001, **** P<0.0001.

¹Imvax, Inc., Philadelphia, PA. ²Department of Radiation Oncology, Weill Cornell Medicine, NY, US.



CONCLUSIONS

• Death in *m*IGV-001 cells correlated both *in vitro* and *in vivo* with the detection of ICD damage-associated molecular patterns (eATP and HMGB1).

• The *m*IGV-001 mechanism of action involves stress-mediated activation of pathways consistent with apoptosis, and induced immune responses specifically detected in the dLNs vs nondraining nodes.

• These data suggest a potential mechanism of action of IGV-001 in GBM via ICD stimulation of an antitumor immune response.

REFERENCES

1. Andrews DW, et al. *Clin Cancer Res.* 2021;27(7):1912-1922. 2. Stupp R, et al. *N Engl J Med*. 2005;352(10):987-996. 3. Zilberberg J, et al. *J Immunother Cancer*. 2021;9:A231-A231. 4. Kroemer G, et al. *Nat Immunol*. 2022;23(4):487–500.



#1071